Load Identification for Structural Health Prognosis

Claus-Peter Fritzen, Maksim Klinkov
Institute of Mechanics and Control Engineering – Mechatronics
and Center of Sensor Systems (ZESS)
University of Siegen
GERMANY

claus-peter.fritzen@uni-siegen.de

ABSTRACT

For purposes of monitoring and damage prognosis another important aspect is to know the external loads which act on a structure. The knowledge of these loads enables us to make an assessment of damage after extreme events and updated forecasts of the remaining life-time. In many practical applications it is not possible to measure the forces e.g. resulting from wind loads or traffic directly. Therefore, these forces are determined indirectly from dynamic response measurements. In this paper, an overview of available time domain load reconstruction methods is presented. An attempt of highlighting the main advantages and disadvantages of different approaches, which are used in engineering is done. The importance of sensors type as well as their locations is discussed. Finally, the methods applicability is shown.

1.0 INTRODUCTION

Aircraft structures, buildings, wind turbines, stadiums (during concerts or football matches) are some of the examples where the dynamics of the structure should be taken into consideration for reliable construction. Especially in the fatigue life assessment of the structure or some of its components, both material properties and load characteristics are essential parameters. Therefore the time history of external forces is an important quantity in the forecasting of the remaining lifetime [1]. In many practical applications the measurement of the external loads is limited or not possible due to sensor limitations or unknown nature of the external forces, see Fig. 1. Even when load measurement transducers are available, they may either alter the system properties (electronic circuits) or intrude the load path (contacts and joint).

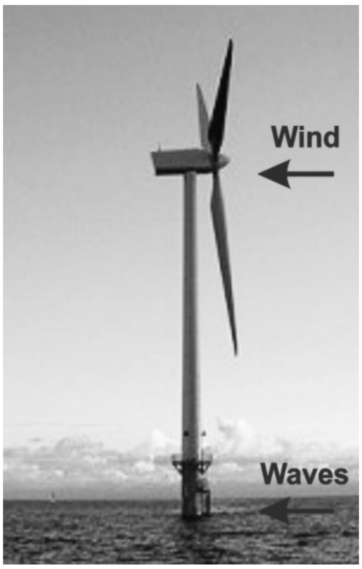

Figure 1: Offshore Wind energy plant under unknown dynamic loads from wind and waves.

The load identification has been studied extensively for the last two decades. Many attempts were made by engineers to solve this problem by using indirect measurement techniques, which include the transformations of related measured quantities such as acceleration, velocity, position or strain. These transformations generally lead to a so-called inverse problem, where system properties and responses are known while excitations are unknown. It is well known that inverse problems are often 'ill-posed' in the mathematical sense, that is one of 1) the existence, 2) the uniqueness, or 3) the stability of solution is violated [2, 3, 4, 5]. If this inversion can be done, the system itself becomes its own force sensor. A variety of methods were elaborated to overcome the above mentioned difficulties for external load estimation in the time and frequency domain ([6] - [13]). Stevens [3] wrote an excellent overview of this topic, which includes some earlier studies on inverse analysis of external forces. Some of these methods are based on the frequency or impulse response functions or use regularization and dynamic programming in the time domain, which was proposed by Trujillo and Busby [14] and applied by Doyle [6]. Others use an integration of measured acceleration signals [7] or can only determine the sum of all forces and moments applied to the center of mass (SWAT), [8]. Most of them require first to record the system responses and then apply the analysis methods for force history reconstruction or insert a time shift for identification of the forces in non-collocated case (sensors and loads positions are not collocated) [2]. Although the indirect measurement of the external load history has been referred to so far, for a full understanding of the force identification it may be required to know: 1) the time history and 2) the locations of the applied forces. Generally all force reconstruction methods that where proposed by mechanical engineers can be summarized in three main groups [10]:

1. Deterministic method: frequency or time domain methods
2. Stochastic method (statistical models)
3. Artificial intelligence-based methods (neural networks)

Here the main focus is on showing certain advantages and disadvantages of the four methods. Three of them have been already extensively used: Inverse Structural Filter (ISF) [2, 13], Partial Modal Matrix technique (PMM) [7], Dynamic Programming (DP) [6, 14]. The fourth one is an Unknown Input Observer approach (UIO), which was proposed by Ha et al. [15, 16] for control purposes and adopted in [17] for external loads and states reconstruction of the structures. While most of these techniques have rigorous mathematical foundation, they are not presented here, details can be found in [2, 6, 13, 14, 15, 17 and 20]. Since all methods given in the literature have their own merits, limitations and drawbacks, applicability is often the decisive factor when choosing a particular method.

2.0 INVERSE ANALYSIS

2.1 Problem Definition

The response of the structure to external forces can often be considered to be linearly dependent on the applied forces. This is the case when the system can be considered to be linear during the excitation process so that the deformations are small enough to neglect geometric nonlinearity. In such case the response $\boldsymbol{y}(t)$ of the structure can be related to the excitation force $\boldsymbol{u}(t)$ by a linear convolution integral in continuous time or by algebraic equations in discrete time:

$$a)\ \boldsymbol{y}(t)=\int_0^t \boldsymbol{h}(t-\tau)\boldsymbol{u}(\tau)d\tau, \qquad b)\ \boldsymbol{y}_k=\sum_{i=0}^{n}\boldsymbol{h}_i\boldsymbol{u}_{k-i}, \qquad c)\ \boldsymbol{Y}(\Delta t)=\boldsymbol{H}(\Delta t)\boldsymbol{U}(\Delta t), \tag{1}$$

where $\boldsymbol{h}(t)$ is the impulse response function IRF and $\boldsymbol{h}_i$ are the Markov parameters of the linear system. The assumption has been made that $\boldsymbol{u}(t)=\boldsymbol{h}(t)=\boldsymbol{y}(t)=\boldsymbol{0}$ for $t<0$. The quantities $\boldsymbol{H}(\Delta t)$, $\boldsymbol{U}(\Delta t)$ and $\boldsymbol{Y}(\Delta t)$ are the transfer matrix, input and measurement vectors respectively and have following construction:

$$\boldsymbol{H}(\Delta t)=\begin{bmatrix} \boldsymbol{H}(\Delta t) & 0 & \cdots & 0 \\ \boldsymbol{H}(2\Delta t) & \boldsymbol{H}(\Delta t) & \ddots & \vdots \\ \vdots & \vdots & \ddots & 0 \\ \boldsymbol{H}(n\Delta t) & \boldsymbol{H}((n-1)\Delta t) & \cdots & \boldsymbol{H}(\Delta t) \end{bmatrix}, \qquad \begin{matrix} \boldsymbol{Y}(\Delta t)=\left[\boldsymbol{Y}(\Delta t) \quad \cdots \quad \boldsymbol{Y}(n\Delta t)\right]^T \\ \boldsymbol{U}(\Delta t)=\left[\boldsymbol{U}(\Delta t) \quad \cdots \quad \boldsymbol{U}(n\Delta t)\right]^T \end{matrix}. \tag{2}$$

If the measurement responses are known then the problem of estimating the time history of external forces is referred as a deconvolution of the above integral. It is obvious that the IRF should be known as well, which leads to another problem of IRF construction either from measurement or from modeling. For sake of simplicity consider the algebraic equation (Eq. 1 *c*). Deconvolution of this equation is an 'ill-posed' problem, the matrix ***H(Δt)*** is ill-conditioned and consequently [18]: a) the system defined in (Eq. 1) can be numerically insolvable, b) if the solution of the (Eq. 1) exists, it may be unstable with regard to small disturbances (measurement noise). The ill-conditioning of the matrix ***H(Δt)*** strongly depends on [18]: 1) the sensor placement, 2) the size of the matrix ***H(Δt)***. Jacquelin et al. [5] has shown that by using the singular value decomposition (SVD) of a matrix ***H(Δt)*** as:

$$\boldsymbol{H}(\Delta t)=\boldsymbol{L\Sigma V}^T=\sum_{i=1}^{n}\boldsymbol{l}_i\sigma_i\boldsymbol{v}_i^T. \tag{3}$$

The ill-conditioning can easily be shown by the solution of (Eq. 1 *c*):

$$\boldsymbol{U}(\Delta t)=\sum_{i=1}^{n}\boldsymbol{v}_i\frac{\boldsymbol{Y}(\Delta t)}{\sigma_i}\boldsymbol{l}_i^T. \tag{4}$$

The ability to solve (Eq. 4) depends on the singular values SV of the matrix ***H(Δt)***. Moreover, by using the SV it is easy to show, that there exist different kinds of ill-conditioning [17]: solely ill-posed or ill-posed and rank-deficient problems. Their nature is based on the SV as well:

- the SV decay gradually to zero with no particular gap: solely ill-posed problem,
- the SV decay gradually to zero and there is a well-determined jump between two SV: ill-posed and rank-deficient problem.

The solely ill-posed problem arises in case when the sensors and forces are collocated. On the contrast the ill-posedness and rank-deficiency appear when the measurements points and the excitation positions are not collocated. This generally means that the first row(s) of the ***H(Δt)*** are filled with zeros, due to time delay, the time that excitation waves need to reach the sensors. The complete problem is even more spoiled by the noise contamination of the measured responses ***Y(Δt)***, which can drive (Eq. 4) to unstable solutions.

2.2 Solution Methods

The above mentioned problems related to the force reconstruction have been solved by several methods. The main principle is based on the conversion of the ill-posed problem into a well-posed one, which is done with the help of different regularization techniques. Below four time domain methods are presented.

2.2.1 Dynamic Programming (DP)

The dynamic programming method is based on the reconstruction of the force history by the least square solution for the first-order state space system. The DP is a recursive algorithm which solves the least square problem in two steps: backward and forward sweep. That means that for a linear time-invariant discrete system (Eq. 5) (here the general state space is extended with $\boldsymbol{u}_{k+1}=\boldsymbol{u}_k+\Delta\boldsymbol{u}_k$):

$$\begin{bmatrix} \boldsymbol{x}_{k+1} \\ \boldsymbol{u}_{k+1} \end{bmatrix} = \begin{bmatrix} \boldsymbol{A} & \boldsymbol{B} \\ \boldsymbol{0} & \boldsymbol{I} \end{bmatrix} \begin{bmatrix} \boldsymbol{x}_{k} \\ \boldsymbol{u}_{k} \end{bmatrix} + \begin{bmatrix} \boldsymbol{0} \\ \Delta \boldsymbol{u}_{k} \end{bmatrix}, \qquad \boldsymbol{y}_k = \boldsymbol{C}\boldsymbol{x}_k + \boldsymbol{D}\boldsymbol{u}_k \tag{5}$$

where: $\boldsymbol{A}$, $\boldsymbol{B}$, $\boldsymbol{C}$ and $\boldsymbol{D}$ are constant matrices, and $\boldsymbol{x}_k$, $\boldsymbol{y}_k$ and $\boldsymbol{u}_k$ are state, output and input vectors at time instance k, respectively. The sequence of $\Delta\boldsymbol{u}_k$ should be found that minimize the regularized squared error function:

$$\boldsymbol{E} = \sum_{k=1}^{n} (\boldsymbol{y}_k - \hat{\boldsymbol{y}}_k)^T \boldsymbol{W}_w (\boldsymbol{y}_k - \hat{\boldsymbol{y}}) + \Delta\boldsymbol{u}_k{}^T \boldsymbol{W}_r \Delta\boldsymbol{u}_k, \tag{6}$$

with the weighting matrices $\boldsymbol{W}_w$ and $\boldsymbol{W}_r$. The $\boldsymbol{W}_r$ can be substituted by a diagonal matrix such as $\boldsymbol{W}_r=\omega\boldsymbol{I}$. An L-curve method is used to pick a right value of ω. This approach allows a good load estimation for time variant or invariant systems as well as for the case when the sensors and forces are not collocated. Apart of the computational effort, the DP has following drawbacks:

- the L-curve method works well only, if the measurements are noise free [5],
- it is not applicable to non-linear systems,
- online load reconstruction is not possible (which means that a complete sequence of measurement signals should be recorded before running the DP algorithm)

2.2.2 Inverse Structural Filter (ISF)

The ISF method estimates the loads history $\boldsymbol{u}$, by means of a non-causal inverse structural filter. The dynamic system is represented in a form of first order state space as:

$$\begin{aligned} \boldsymbol{x}_{k+1} &= \boldsymbol{A}\boldsymbol{x}_k + \boldsymbol{B}\boldsymbol{u}_k \\ \boldsymbol{y}_k &= \boldsymbol{C}\boldsymbol{x}_k + \boldsymbol{D}\boldsymbol{u}_k \end{aligned}. \tag{7}$$

The Markov parameters $\boldsymbol{h}_i$, see (Eq. 1b), which can be obtained analytically or from physical test are related to the state space matrices as follows: $\boldsymbol{h}_0 = \boldsymbol{D}$, $\boldsymbol{h}_i = \boldsymbol{C}\boldsymbol{A}^{i-1}\boldsymbol{B}$, and i=1,2…n. Manipulation of (Eq. 7), in order to interchange the input and output, yields the inverse structural system:

$$\begin{aligned} \boldsymbol{x}_{k+1} &= \hat{\boldsymbol{A}}\boldsymbol{x}_k + \hat{\boldsymbol{B}}\boldsymbol{y}_k \\ \boldsymbol{u}_k &= \hat{\boldsymbol{C}}\boldsymbol{x}_k + \hat{\boldsymbol{D}}\boldsymbol{y}_k \end{aligned} \quad \text{where:} \quad \begin{aligned} &\hat{\boldsymbol{A}} = [\boldsymbol{A} - \boldsymbol{B}\boldsymbol{D}^{+}\boldsymbol{C}], \quad \hat{\boldsymbol{B}} = \boldsymbol{B}\boldsymbol{D}^{+}, \\ &\hat{\boldsymbol{C}} = -\boldsymbol{D}^{+}\boldsymbol{C}, \quad \hat{\boldsymbol{D}} = \boldsymbol{D}^{+}, \end{aligned} \quad \text{and} \quad \boldsymbol{u}_k = \sum_{i=0}^{n} \boldsymbol{r}_i \boldsymbol{y}_{k-i}. \tag{8}$$

Here, $\boldsymbol{r}_i$ are the filter coefficients (inverse system Markov parameters) and n is the size of that filter. The Moore-Penrose pseudo-inverse $\boldsymbol{D}^{+}$ requires that $\boldsymbol{D}$ in (Eq. 8) has full column rank, or in other words that the number of sensors should be bigger or equal than the number of excitation forces. The presence of the feed-through matrix $\boldsymbol{D}$ requires first: usage of accelerometers as measuring devices, second: the accelerometer sensors should be positioned at the same location as the excitation forces (except, modal models are used). When these two requirements are not satisfied the matrix $\boldsymbol{D}$ vanishes. For this case the system should be stepped forward in time by l steps. The step l is a non-causal lead which accounts the time of wave propagation from the source to the sensor. This lead stabilizing the inverse problem by removing the zero rows from the transfer matrix $\boldsymbol{H}(\Delta t)$, so that the ISF has following form:

$$\boldsymbol{u}_k = \sum_{i=0}^{n} \boldsymbol{r}_i \boldsymbol{y}_{k+l-i}. \tag{9}$$

The filter coefficients then calculated using a least square:

$$\boldsymbol{R} = [\underbrace{\boldsymbol{0} \quad \cdots \quad \boldsymbol{0}}_{l}\, \boldsymbol{I}\, \underbrace{\boldsymbol{0} \quad \cdots \quad \boldsymbol{0}}_{n-l-1}]\boldsymbol{H}^{+}, \qquad \text{with:} \qquad \boldsymbol{R} = [\boldsymbol{r}_0 \quad \cdots \quad \boldsymbol{r}_n], \tag{10}$$

where $\boldsymbol{H}^{+}$ is a pseudo-inverse of the Markov matrix [13]. The beauty of this method is that the pseudo-inverse needs to be calculated only once. This approach enables an almost online load reconstruction for time invariant systems as well as loads estimation in the case when the sensors and excitation positions are not the same. An individual sensor lead was proposed by [2] as an extension of this method. In summary, the disadvantages are:

- the difficulties of choosing a proper non-causal lead l;
- high sensitivity to the measurement noise;
- non-applicability to nonlinear systems.

2.2.3 Partial Modal Matrix (PMM)

The PMM method is an extension of the SWAT (Sum of Weighted Acceleration Techniques) and based on inversion of the partial mode shape matrix. This method required the knowledge of the mode shapes at all input and sensor locations. The modal coordinates allows one to use the non-collocated alignment of sensors and input forces positions.

The force estimation is done as:

$$\boldsymbol{f}(t) = (\boldsymbol{X}^{T})^{+}\left\{\boldsymbol{f}_I(t) + \boldsymbol{f}_D(t) + \boldsymbol{f}_E(t)\right\}, \quad \text{with: } \boldsymbol{f}_I(t) = \boldsymbol{\eta}\ddot{\boldsymbol{q}}, \quad \boldsymbol{f}_D(t) = \boldsymbol{\beta}\dot{\boldsymbol{q}}, \quad \boldsymbol{f}_E(t) = \boldsymbol{\Lambda\eta q}. \tag{11}$$

Here, the $\boldsymbol{f}_I$, $\boldsymbol{f}_D$ and $\boldsymbol{f}_E$ are the vectors of modal inertia, modal damping and modal elastic forces; the $(\boldsymbol{X}^T)^{+}$ is a pseudo inverse of the transposed modal matrix $\boldsymbol{X}$ and $\boldsymbol{f}(t)$ is a vector of external forces; $\ddot{\boldsymbol{q}}$, $\dot{\boldsymbol{q}}$, $\boldsymbol{q}$ are the generalized acceleration, velocity and displacement vectors. The inverse problem is solved in three main steps:

1) Based on the accelerometer measurements at r locations, the velocities and displacements are calculated by successive integration. ($\ddot{\boldsymbol{x}}$, $\dot{\boldsymbol{x}}$, $\boldsymbol{x}$)
2) Some modes n_s are chosen, and generalized accelerations, velocities and displacements corresponding to these modes are calculated: $\ddot{\boldsymbol{q}}(t) = \boldsymbol{X}^{+}\ddot{\boldsymbol{x}}(t)$, $\dot{\boldsymbol{q}}(t) = \boldsymbol{X}^{+}\dot{\boldsymbol{x}}(t)$, $\boldsymbol{q}(t) = \boldsymbol{X}^{+}\boldsymbol{x}(t)$. Here the number of modes n_s cannot exceed the number of sensors r.
3) Finally $\boldsymbol{f}(t)$ is determined by (Eq. 11). Here the number of inputs n_i cannot exceed the number of modes n_s.

The PMM approach is applicable only when the complete measurements are at hand. The main drawback of PMM is that the pseudo-inverse requires big instrumentation for good load estimation $r \geq n_s \geq n_i$.

2.2.4 Unknown Input Observer (UIO)

The UIO is a time domain approach, which originally was invented for control engineering purposes [15, 16]. It allows simultaneous reconstruction of the inputs and states (velocities, positions) of a linear or nonlinear time invariant system. The main principle is based on the construction of the observer for a general first order nonlinear state space system:

$$\begin{aligned} \dot{x}(t) &= \boldsymbol{A}\boldsymbol{x}(t) + \boldsymbol{B}\boldsymbol{u}(t) + \boldsymbol{f}((\boldsymbol{x},\boldsymbol{u}),\boldsymbol{y}) \\ \boldsymbol{y}(t) &= \boldsymbol{C}\boldsymbol{x}(t) + \boldsymbol{D}\boldsymbol{u}(t) \end{aligned}, \tag{12}$$

where $\boldsymbol{x}(t)$, $\boldsymbol{u}(t)$ and $\boldsymbol{y}(t)$ are the states, unknown inputs and measured outputs, respectively. Matrices $\boldsymbol{A}$, $\boldsymbol{B}$, $\boldsymbol{C}$ and $\boldsymbol{D}$ are real, constant and of appropriate dimensions. $\boldsymbol{f}(.)$ is a real nonlinear vector function. The proposed observer has the following form [15]:

$$\begin{aligned} \dot{\omega}(t) &= \boldsymbol{N}\omega(t) + \boldsymbol{L}\boldsymbol{y}(t) + \boldsymbol{T}\,\boldsymbol{f}_L(\hat{\xi},\boldsymbol{y}) \\ \hat{\xi}(t) &= \omega(t) + \boldsymbol{Q}\boldsymbol{y}(t) \end{aligned}, \qquad \text{with:} \qquad \xi(t) = \begin{bmatrix} \boldsymbol{x}(t) \\ \boldsymbol{u}(t) \end{bmatrix}. \tag{13}$$

An appropriate set of observer matrices $\boldsymbol{N}$, $\boldsymbol{L}$, $\boldsymbol{T}$ and $\boldsymbol{Q}$ should be found, so that the error between the estimated inputs and states and the real one will converge to zero as the time evolves. It is possible to find these matrices with the help of a linear matrix inequality (LMI) technique [19]. There are still two assumptions in this method that should be satisfied: the $\boldsymbol{D}$ matrix must have full column rank (this means that acceleration sensors have to be used); the number of sensors should be bigger or equal to the number of unknown inputs plus the number of nonlinear terms. Once the observer matrices are calculated, the inputs and states can be reconstructed simultaneously online. The ability of online reconstruction and inherited noise robustness make the UIO very attractive for external load estimation. One of the main drawbacks of this method is that it works only for invariant systems.

A comprehensive discussion of the UIO with respect to the application of force reconstruction is given in [20].

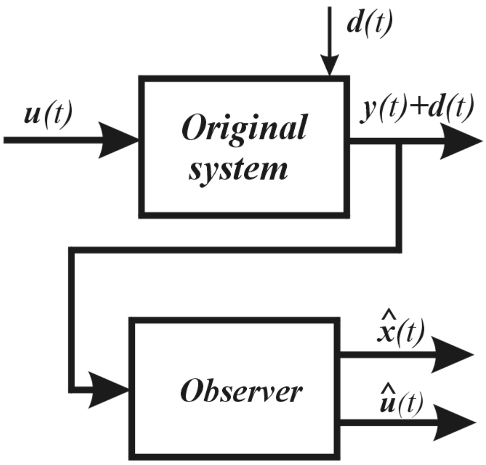

Figure 2: Scheme of state and input estimator structure for a class of nonlinear systems.

3.0 EXPERIMENTAL SETUP AND RESULTS

For the verification of the proposed UIO method a special structure that should represent a scaled tower and foundation of a wind energy plant was built (see Figure 3 left). The tripod is welded from steel pipes of the diameters (37.2 *mm* and 21.3 *mm*) and fixed to the concrete foundation with four bolts at each leg (see Figure 3 left). The load was exerted on the tower with the help of a wind fan which was blowing on to aluminum plate. Between the plate and supporting beam which in its turn was rigidly connected to the tower, a force sensor was located for later validation of the force estimated by means of the observer. For data acquisition two types of sensors (a bi-axial accelerometer and two strain gauges) were used. These data was then fed into the observer that was calculated on the basis of the FE model (see Figure 3 right). The initial FE model was improved using model-updating techniques, converted into modal coordinates and finally transformed into state space notation. The thick black spots on the model (see Figure 3 right) represent the locations of the accelerometer (top) and strain gauge (bottom) respectively.

In the first step the obtained observer was tested in the Simulink/Matlab environment under different conditions. Mainly three questions were subject of these simulations:

1. How the complexity of the calculated observer (the number of modes which are included in the state space model) influences the reconstruction of external force?
2. How much the noise level of each sensor changes the observer performance?
3. Does the shift of the acceleration sensor location from the point where the force was applied still preserve the stable load reconstruction (collocation problem)?

For the simulations, the original system (see Figure 3) has been built from the FE model consisting of the first 30 mode shapes. The set of observers with 8, 10, 12 and 14 modes in which only the bending modes were included in both (x and y) directions was calculated whereas the force was applied only in x direction.

Each of these observers then was tested for increasing noise level on one of the sensors (strain gauge or accelerometer) when the noise on the other sensors has been kept constant and was equal to 2%. In Figure 4 the relative error behavior between the 30 modes system (assumed to be an original system) and the reconstructed force for the observers with different number of modes is shown. Here the acceleration sensor was collocated with the position of the applied force.

The relative error as well as the noise level was measured by the relative discrepancy $\mathcal{D}$:

$$\mathcal{D}_{relative} = 100\sqrt{\frac{\sum\left(Signal_{exact} - Signal_{noisy}\right)^2}{\sum Signal_{exact}{}^2}} \tag{14}$$

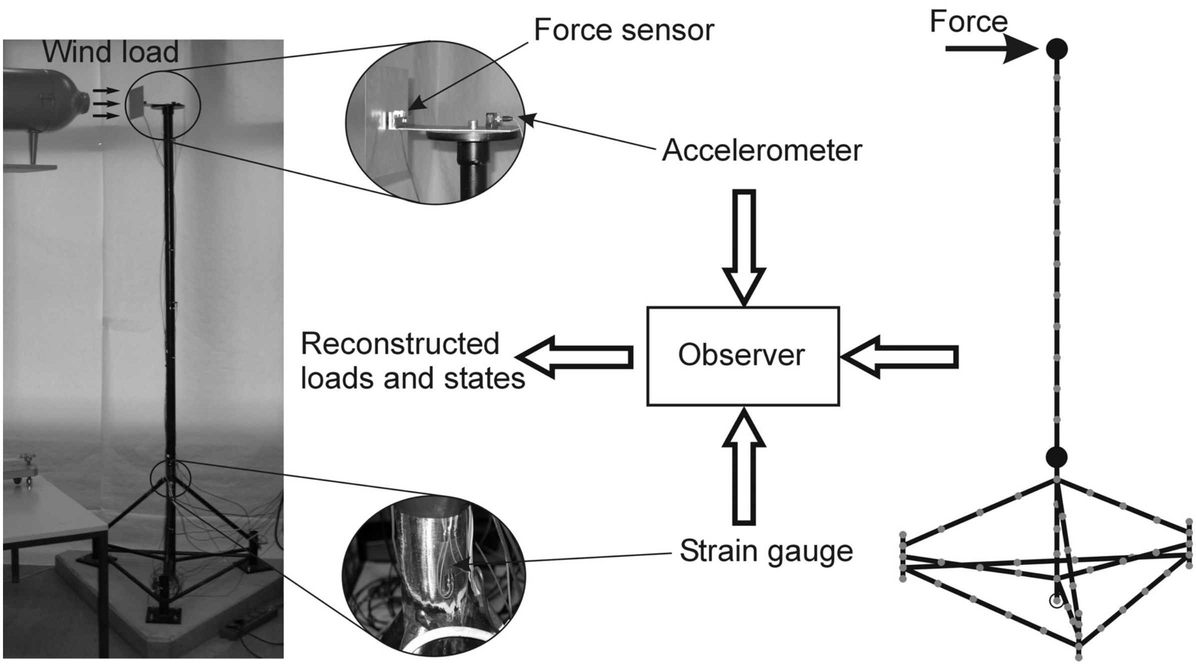

Figure 3: Laboratory test right (left) and FE model of the structure (right).

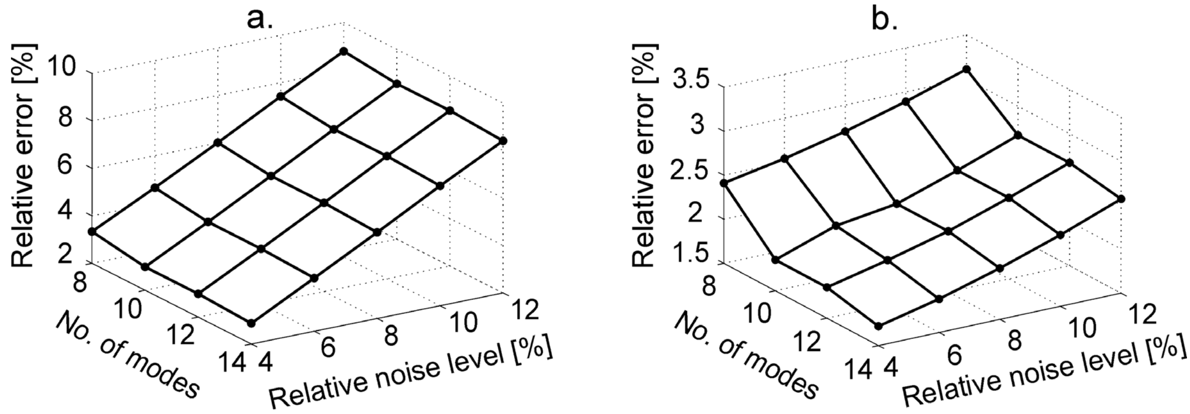

Figure 4: Relative simulated error of estimated force for different number of modes and (a) – relative noise level of strain gauge (b) – relative noise level of the collocated accelerometer and force.

The load for all simulations was a unit force that was applied for 3 seconds at a single node on top (see Figure 3) in one direction described as (using Matlab functions):

$$\boldsymbol{F}(t) = 200\,\boldsymbol{sin}(2\pi t \cdot 2Hz) + 20\,\boldsymbol{square}(2\pi t \cdot 30Hz) + 10\,\boldsymbol{sawtooth}(2\pi t \cdot 220Hz) \qquad (15)$$

The same pattern of excitation as well as the noise variations was applied for the case when the accelerometer was shifted by one node down (0.13 meter) from the force location. Figure 5 presents the observer performance for that case. Both figures show that the presence and increase of the noise especially in the strain gauge leads to higher deviation of the estimated load from the real one.

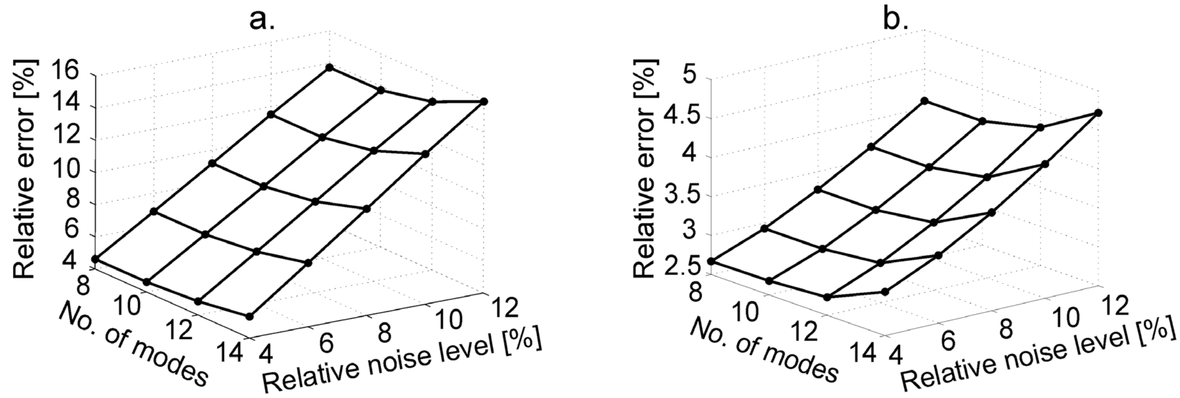

Figure 5: Relative simulated error of estimated force for different number of modes and (a) – relative noise level of strain gauge (b) – relative noise level of the non-collocated accelerometer and force.

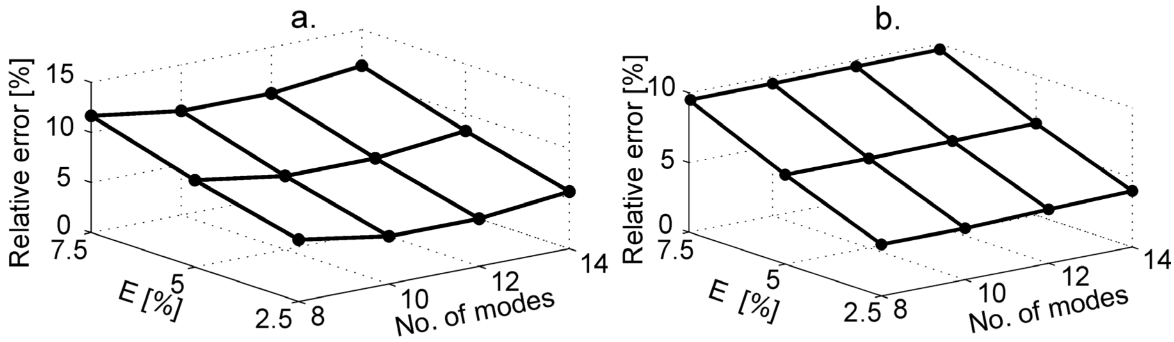

Figure 6: Relative simulated error of the estimated force for different number of modes and relative change of the global Young's modulus E. (a) – collocated force and accelerometer (b) – non-collocated force and accelerometer.

On the other hand the noise contamination of the acceleration signals does not lead to the strong force perturbation. There is an important difference between collocated and non-collocated observer behavior that can be noticed form Figures 4 and 5. The performance of the collocated observer is slightly improving as the observer size increases (higher number of modes included) whereas in the non-collocated case it shows the opposite tendency. This behavior can be due to weaker measured signals (either strain or acceleration) especially for higher modes of vibration which leads to the stronger oscillations of the estimated force. Change of the original system dynamics (shift of the eigenfrequencies) due to the environmental conditions (temperature variation, marine growth), was considered by another simulation test. Here the global Young's modulus was varied from original one by 2.5%, 5% and 7.5% which led to the change of the natural frequencies. The performance of the observer with noise level in both sensors equal to 2% is presented in Figure 6 for both collocated and non-collocated cases. These results clearly show that the increase of the complexity of the observer does not necessarily improve the force estimation.

Another issue which also can be noticed from Figure 6 is that the non-collocated observer is less sensitive to the changes of original system.

Finally a collocated observer using 8 modes was tested on a laboratory structure. The acquired measurement data which was directly fed into observer is shown in Figure 7 (a, b). One can see that the noise level of the strain gauge is very high which leads to strong perturbation of the reconstructed force in the steady state (up to 2.5 seconds) that is overlapped with the measured force in Figure 7 (c). Nevertheless the real force was estimated well after the fan was switched on (see Figure 7 c magnification). The relative error between the estimated and measured external force was 11.5% (where the error is 100 $||f_{est}\text{-}f_{meas}||_2 \,/\, ||f_{meas}||_2$). Some signal preprocessing was necessary, especially removing the offset from the acceleration and strain signals which is always present even if the structure is in steady state.

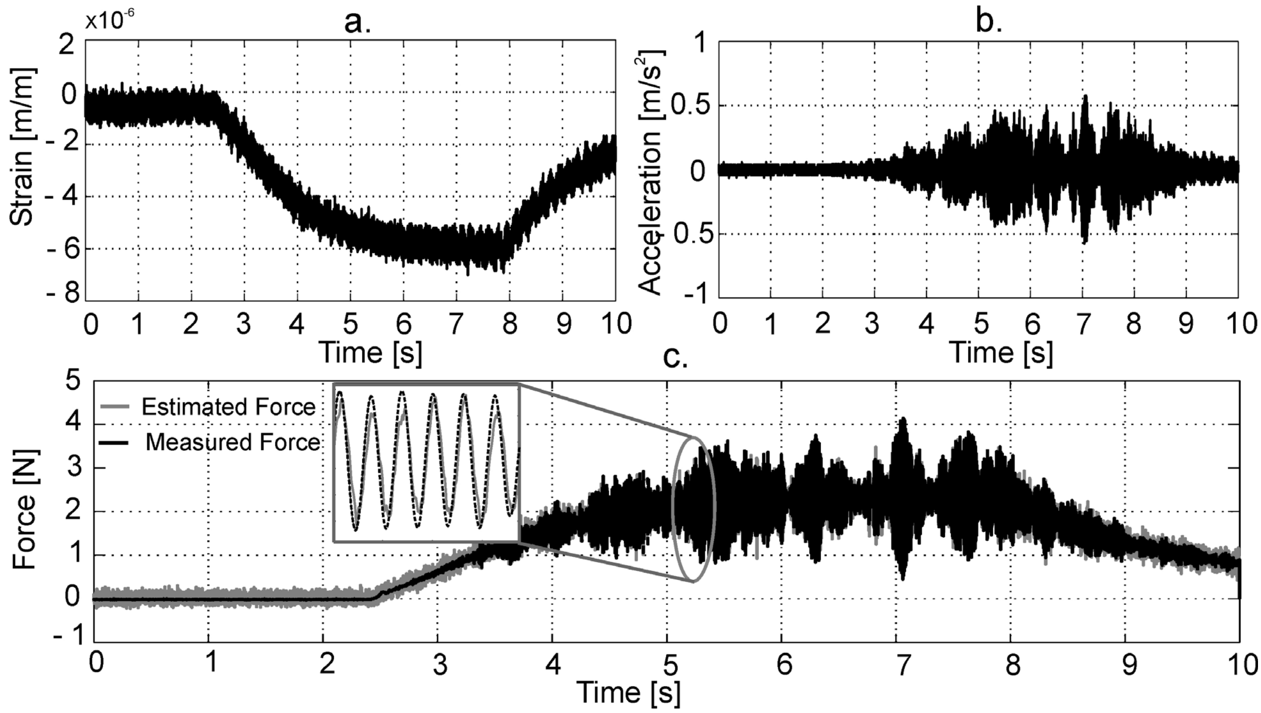

Figure 7. Measured signals and estimated force for external wind load applied on the laboratory structure in *x* direction. (a) – strain, (b) – acceleration, (c) – force.

4.0 CONCLUSION

All methods considered in this paper try to overcome ill-conditioning of the inverse problem by either regularization (Tikhonov, SVD truncation and so on), or transformation of the ill-posed problem into a well-posed one. All of them are based on the knowledge of mathematical or identified models. This requires modeling or system identification as first step for load estimation. The load locations are also assumed to be known a priori for all of them. The DP approach is a good and reliable technique for both, time invariant and time variant systems, and works well also when the sensor signals are polluted with noise. Nevertheless its implementation is rather complicated. Together with the recursive algorithm it is not applicable for online load estimation. The ISF and UIO have the ability for online load reconstruction. The ISF can be easily implemented but requires individual sensor shifts for the non-collocated problem and is very sensitive to measurement noise. The UIO has better behavior than the ISF when the noise level is high. Apart of this the UIO is also suited for nonlinear systems and can be applied for non-collocated problems in case when modal coordinates are used. The PMM is an off-line approach; it does not suffer from the non-collocation because it uses modal models. Although the pseudo inverse, which is done twice in PMM requires that the number of inputs does not exceed the number of modes for a first inversion and the number of modes should be less than the number sensors for the second inversion. As a consequence a complicated instrumentation is needed for good force reconstruction and can be considered as a big disadvantage, especially in the case when several loads should be estimated. A comparison of the four methods for time domain load reconstruction revealed that all methods have their own merits, limitations and drawbacks. Therefore the application is the decisive factor when choosing a particular method.

The unknown input observer was then applied to a laboratory structure of the WEP for external force reconstruction. The set of observers has been designed using an LMI for different numbers of modes; prior knowledge of the structure as well as the force location was available for the FEM. With the help of this set the behavior of the observer was validated with respect to noise contamination level and model variation.

The observers show a good estimation of the real/simulated force and are very robust to noisy measurements, although their performance depended on the accuracy of the model, noise level of the measurements and the sensor allocations. The 8 modes observer performance was finally validated on a real structure.

5.0 REFERENCES

[1] P. Johannesson: *Rainflow analysis of switching Markov loads,* PhD thesis, Lund Institute of Technology, Denmark (1999).

[2] L.J.L. Nordström: *Input estimation in structural dynamics*, PhD thesis, Chalmers University of Technology Sweden, Göteborg, Sweden (2005).

[3] K. Stevens: *Force identification problems - an overview*, Proc. of SEM, Spring Meeting, Houston, (1987), pp. 838-844.

[4] H. Inoue, J.J. Harrigan & S.R. Reid: *Review of inverse analysis for indirect measurement of impact force*, Applied Mechanics Reviews, Vol. 54, (2001), pp. 503-524.

[5] E. Jacquelin, A. Bennani, P. Hamelin: *Force reconstruction and regularization of a deconvolution problem*, Journal of Sound and Vibration, Vol. 265, (2003), pp. 81-107.

[6] J.F Doyle, R. Adams: *Multiple force identification for complex structures*, Experimental Mechanics, Vol. 42(1), (2002), pp. 25 -36.

[7] G. Ginaro, A. Domingos: *Input force identification in time domain*, Proc. of 16th IMAC, Santa Barbara, California, USA (1998), pp. 124 – 129.

[8] T.G. Carne, V.I. Bateman, R.L. Mayes: *Force reconstruction using a sum of weighted accelerometers technique*, Proc. of 10th IMAC, San Diego, California, USA (1992), pp. 291 – 298.

[9] X.L. Guo, D.S. Li: *Experimental study of structural random loading identification by the inverse pseudo excitation*, Structural Engineering and Mechanics, Vol.18, (2004), pp. 791 – 806.

[10] T. Uhl, P. Macej: *Load identification with use of neural networks – design and application*, Mechanical Systems and Signal Processing, (2006).

[11] D. Söffker, I. Krajcin: *Modified PIO design for robust unknown input estimation*, ASME DETC Conferences, Chicago, Illinois, USA (2003).

[12] R. Seydel, F.K. Chang: *Impact identification if stiffened composite panels*, Smart Materials and Structures, Vol. 10, (2001), pp. 354-379.

[13] A.D. Steltzner, D.C. Kammer. *Input force estimation using an inverse structural filter*. Proc. of 17th IMAC, Kissimmee, Florida, USA (1999), pp. 954-960.

[14] D.M. Trujillo, H.R. Busby: *Practical inverse analysis in engineering*, New York, CRC Press, (1997).

[15] Q.P. Ha, H. Trinh: *State and input simultaneous estimation for a class of nonlinear systems*, Automatica, Vol. 40, (2004), pp. 1779-1785.

[16] Q.P. Ha, A.D. Nguyen, H. Trinh: *Simultaneous state and input estimation with application to a two-link robotic system*, Proc. ASCC of the 5th Asian Control Conference, (2004), pp. 322-328.

[17] M. Klinkov, C.P. Fritzen: *Online estimation of external loads from dynamic measurement*, Proc. ISMA, Leuven, Belgium (2006), pp. 3957-3968.

[18] P.C. Hansen: *Rank deficient and discrete ill-posed problems*, SIAM, Philadelphia, PA, 1998.

[19] S. Boyd, L. El Ghaoui, E. Feron, V. Balakrishnan: *Linear Matrix Inequalities in Systems and Control Theory*, SIAM books, Philadelphia, (1994).

[20] C.-P. Fritzen, M. Klinkov, P. Kraemer: Vibration-based Damage Diagnosis and Monitoring of External Loads, in Ostachowicz W., Guemes, A (Eds.) New Trends in Structural Health Monitoring, CISM Lecture Notes No. 542, Springer, pp. 149-208, (2013).